

Kinetics of the CN + HCNO Reaction

Wenhui Feng and John F. Hershberger*

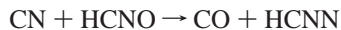
Department of Chemistry and Molecular Biology, North Dakota State University, Fargo, North Dakota 58105

Received: August 3, 2006; In Final Form: September 5, 2006

The kinetics of the CN + HCNO reaction were studied using laser-induced fluorescence and infrared diode laser absorption spectroscopy. The total rate constant was measured to be $k(T) = (3.95 \pm 0.53) \times 10^{-11} \exp[(287.1 \pm 44.5)/T] \text{ cm}^3 \text{ molec}^{-1} \text{ s}^{-1}$, over the temperature range 298–388 K, with a value of $k_1 = (1.04 \pm 0.1) \times 10^{-10} \text{ cm}^3 \text{ molec}^{-1} \text{ s}^{-1}$ at 298 K. After detection of products and consideration of secondary chemistry, we conclude that NO + HCCN is the only major product channel.

1. Introduction

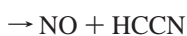
Fulminic acid, HCNO, has recently been identified as an important intermediate in the NO-reburning process for the reduction of NO_x pollutants from fossil-fuel combustion emissions.¹ As a result, the subsequent chemistry of HCNO is of great interest in the overall NO-reburning mechanism. The first experimental kinetic measurement on fulminic acid was recently reported for the reaction of HCNO with OH radicals.² This is a fast reaction with a rate constant of $3.39 \times 10^{-11} \text{ cm}^3 \text{ molec}^{-1} \text{ s}^{-1}$ and produces primarily CO + H₂NO and HCO + HNO products. CN radicals are formed in the oxidation of HCN by OH radicals, which is also an important part of NO_x formation mechanisms in both fuel-rich hydrocarbon flames and flames containing fuel nitrogen. In this paper we present a study of the kinetics of the reaction of CN radicals with HCNO. The reaction has numerous possible product channels, of which the following is only a subset of likely possibilities:



$$\Delta H_f^{298} = -256.9 \text{ kJ/mol} \quad (1a)$$



$$\Delta H_f^{298} = -258.1 \text{ kJ/mol} \quad (1b)$$



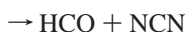
$$\Delta H_f^{298} = -32.4 \text{ kJ/mol} \quad (1c)$$



$$\Delta H_f^{298} = -343.5 \text{ kJ/mol} \quad (1d)$$



$$\Delta H_f^{298} = -428.9 \text{ kJ/mol} \quad (1e)$$



$$\Delta H_f^{298} = -89.6 \text{ kJ/mol} \quad (1f)$$



$$\Delta H_f^{298} = -19.4 \text{ kJ/mol} \quad (1g)$$



$$\Delta H_f^{298} = -7.2 \text{ kJ/mol} \quad (1h)$$



$$\Delta H_f^{298} = -122.5 \text{ kJ/mol} \quad (1i)$$



$$\Delta H_f^{298} = -122.5 \text{ kJ/mol} \quad (1j)$$

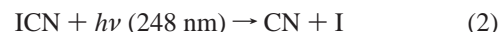


$$\Delta H_f^{298} = -108.6 \text{ kJ/mol} \quad (1k)$$

Thermochemical information has been obtained from standard tables³ as well as other references for the heats of formation of HCNO and NCO,⁴ HCNN,⁵ HCCO,⁶ NCCO,⁷ and CCO.⁸

2. Experimental Section

Total rate constants were measured by both laser-induced fluorescence (LIF) and infrared diode laser absorption methods, as described in a previous publication.² CN radicals were created by 248 nm excimer laser photolysis of ICN:



For the LIF measurements, 248 nm light from an excimer laser (Lambda Physik, Compex 200) was made collinear with 387.088 nm probe light from a frequency doubled Nd:YAG-pumped dye laser (Continuum). Both beams entered a 91.4 cm reaction cell. Laser-induced fluorescence of CN on the $\text{B}^2\Sigma^+ \leftarrow \text{X}^2\Sigma^+$ transition passed through a 400–500 nm band-pass filter and a 385 nm long-pass filter, and was detected at right angles from the laser beams with a PMT mounted against a side window. Signals were recorded on a gated integrator (with 150 ns delay, 200 ns gate width), digitized, and stored on a computer. Timing between excimer and dye pulses was controlled by a computer-controlled digital delay generator. The pump–probe delay was varied to obtain the CN concentration vs time profiles.

Reaction products as well as CN reactants were detected by infrared diode laser absorption spectroscopy. Several lead salts diode lasers (Laser Components) operating in the 80–110 K temperature range were used to provide tunable infrared probe laser light. The IR beam was collimated by a lens and combined with the UV excimer light by means of a dichroic mirror, and both beams were co-propagated through a 1.43 m absorption cell. After the UV light was removed by a second dichroic mirror, the infrared beam was then passed into a $1/4$ m monochromator and focused onto a 1 mm InSb detector (Cincinnati Electronics, $\sim 1 \mu\text{s}$ response time). Transient infrared absorption signals were recorded on a LeCroy 9310A digital oscilloscope and transferred to a computer for analysis. To account for small probe laser thermal deflection effects, signals were collected with the diode laser slightly detuned off the absorption lines, and such transients were subtracted from the on-resonant transients. This is only a minor correction (~ 2 –10%).

HCNO samples were synthesized as previously described^{2,9,10,11} by flash vacuum pyrolysis of 3-phenyl-4-oximinoisoxazol-5(4H)-one. The purity of the HCNO samples was characterized by FT-IR spectroscopy and was typically 95% pure or better, with only small CO₂ and HNCO impurities.

Because HCNO has poor long-term stability, samples were kept at 77 K except when filling the reaction cell. In general, HCNO could be allowed to stand at room temperature for ~ 5 min in our Pyrex absorption cell with minimal decomposition, but significant decomposition over ~ 5 min was commonly observed if the sample was in contact with stainless vacuum lines. As a result, the vacuum system was modified to minimize (but not entirely eliminate) exposure of HCNO to metal.

ICN (Aldrich) was purified by vacuum sublimation to remove dissolved air. SF₆ and CF₄ (Matheson) were purified by repeated freeze–pump–thaw cycles at 77 K and by passing through an Ascarite II column to remove traces of CO₂. NO (Matheson) and ¹⁵N¹⁸O (Isotec) were purified by repeated freeze–pump–thaw cycles at 153 K to remove NO₂ and N₂O. ¹⁵N¹⁸O and ¹⁸O₂ (Isotec) were additionally purified by passing through an Ascarite II column in order to remove trace amounts of ¹⁶O¹²C¹⁸O and ¹⁸O¹²C¹⁸O.

The following molecules were probed using infrared diode laser absorption spectroscopy:

CN ($\nu=1 \leftarrow \nu=0$)	R(7) at 2071.409 cm ⁻¹
HCNO (0100 ⁰ 0) \leftarrow (0000 ⁰ 0)	R(10) at 2203.851 cm ⁻¹
CO ($\nu=1 \leftarrow \nu=0$)	R(11) at 2186.639 cm ⁻¹
N ₂ O (00 ⁰ 1) \leftarrow (00 ⁰ 0)	P(23) at 2202.744 cm ⁻¹
NO ($\nu=1 \leftarrow \nu=0$)	R(10.5) at 1912.072 cm ⁻¹
HNO (100) \leftarrow (000)	P(6) at 2667.785 cm ⁻¹
HCCO ($\nu_2, k=0$) ($\nu=1 \leftarrow \nu=0$)	R(12) at 2031.593 cm ⁻¹
¹⁶ O ¹² C ¹⁸ O (00 ⁰ 1) \leftarrow (00 ⁰ 0)	P(13) at 2322.089 cm ⁻¹
¹⁸ O ¹² C ¹⁸ O (00 ⁰ 1) \leftarrow (00 ⁰ 0)	R(12) at 2322.568 cm ⁻¹

The HITRAN molecular database was used to locate and identify the spectral lines of NO, CO, N₂O, and CO₂ product molecules.¹² Other published spectral data were used to locate and identify CN,^{13,14} HNO,¹⁵ HCNO,¹⁶ and HCCO¹⁷ lines. The spectral lines used are near the peak of the rotational Boltzmann distribution, minimizing sensitivity to small heating effects.

Typical experimental conditions were $P(\text{HCNO}) = 0.2$ Torr, $P(\text{ICN}) = 0.1$ Torr, $P(\text{SF}_6)$ or $P(\text{CF}_4) = 1.00$ Torr, $P(\text{NO}$ or $^{15}\text{N}^{18}\text{O}) = 0.0\text{--}2.00$ Torr, and excimer laser pulse energies of 5 mJ (fluence of ~ 18 mJ/cm²). CF₄ buffer gas was used for CO detection, while SF₆ buffer gas was used for detection of all other product molecules. The choice of buffer gas was motivated by the desire to relax any nascent vibrationally excited product molecules to a Boltzmann distribution.^{18,19}

3. Results

3.1. Total Rate Constants. Measurement of total rate constants of the title reaction at room temperature were performed using both infrared absorption and laser-induced fluorescence, yielding identical results. LIF was used exclusively for experiments at elevated temperatures. Figure 1 shows transient infrared absorption signals of the CN radical, obtained with and without HCNO reagent. Figure 2 shows a plot of CN radical LIF signal as a function of excimer-probe delay time. As both figures show, in the absence of HCNO reagent, a ~ 15 ms⁻¹ decay rate over the time range 10–200 μ s is observed. This decay is attributed to removal of CN radicals by pathways other than the title reaction, including self-reaction, recombina-

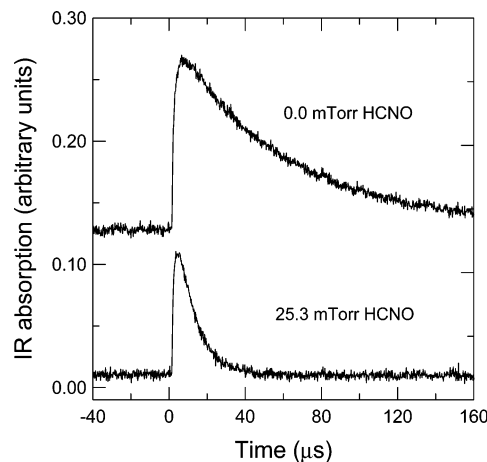


Figure 1. Diode infrared absorption signal of CN as a function of time. Upper trace: 0.0 Torr HCNO; lower trace, 0.0253 Torr HCNO. Other reaction conditions: $P(\text{ICN}) = 0.10$ Torr, $P(\text{SF}_6) = 1.0$ Torr.

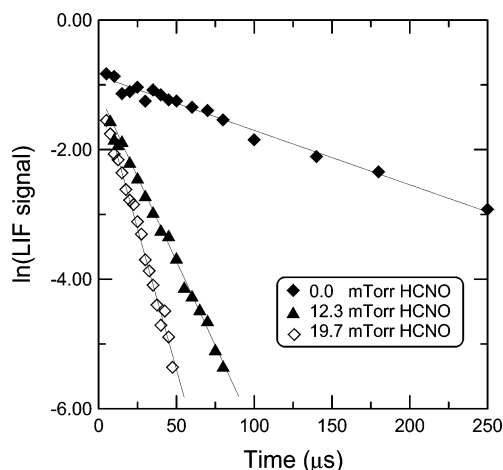


Figure 2. Natural log of the CN laser-induced fluorescence signal as a function of time. Diamonds, 0.0 Torr HCNO; triangles, 0.0123 Torr HCNO; hollow diamonds, 0.0197 Torr HCNO. Other reaction conditions: $P(\text{ICN}) = 0.10$ Torr, $P(\text{SF}_6) = 1.0$ Torr.

tion with iodine atom, reaction with trace of O₂, and diffusion out of the probed region of the reaction cell. Upon the addition of HCNO reagent, a very large increase in CN decay rate is observed. Decay curves such as those shown in Figures 1 and 2 were fit to a single-exponential decay function. Figure 3 shows the resulting decay rates as a function of HCNO pressure, obtained at several different temperatures using LIF detection. A linear dependence is observed, as is expected under the pseudo-first-order kinetics conditions, in which $[\text{HCNO}]_0 \gg [\text{CN}]_0$. As per a standard kinetic treatment, the slope of this plot is the desired bimolecular rate constant k_1 .

Figure 4 shows an Arrhenius plot for the CN + HCNO reaction. Measurements were limited to a rather narrow temperature range of 298–388 K because HCNO decomposition in the reaction cell becomes unacceptably rapid at high temperatures.² Nevertheless, the temperature range is sufficient to obtain reasonably precise Arrhenius parameters. We obtain the following rate constants (error bars represent one standard deviation):

$$k_1(T) = (3.95 \pm 0.53) \times 10^{-11} \exp [(287.1 \pm 44.5)/T] \text{ cm}^3 \text{ molec}^{-1} \text{ s}^{-1}$$

$$k_1(298) = (1.04 \pm 0.1) \times 10^{-10} \text{ cm}^3 \text{ molec}^{-1} \text{ s}^{-1}$$

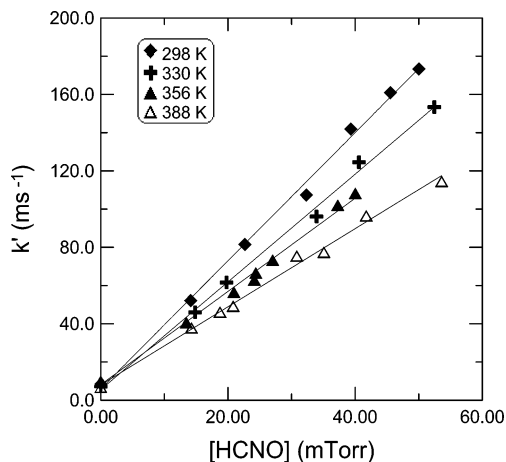


Figure 3. Pseudo-first-order decay rate constant of the CN radical as a function of HCNO pressure. Reaction conditions: $P(\text{ICN}) = 0.10$ Torr, $P(\text{SF}_6) = 1.0$ Torr, $P(\text{HCNO}) = \text{variable}$.

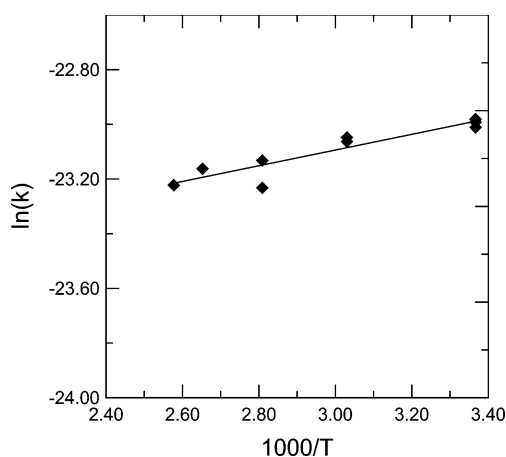


Figure 4. Arrhenius plot for the CN + HCNO reaction.

The negative activation energy observed in this reaction is typical of radical–radical reaction kinetics, and it suggests that the reaction proceeds by complex formation, followed by possible rearrangement and decomposition to form products. A direct hydrogen abstraction mechanism would be expected to have a significant positive activation energy barrier, and it is apparently not a significant contribution in this reaction.

We did not investigate any possible pressure dependence of the rate constant, but the large value obtained at the low pressures used in these experiments indicates that any pressure dependence must be very slight.

3.2. Product Yields. Infrared diode laser absorption was used to attempt detection of NO, N₂O, CO, CO₂, HNO, and HCCO products. Some transient signals are shown in Figures 5–7. All detection experiments were conducted at 298 K. A key point is that many of the same products produced by the title reaction may also be produced through 248 nm photolysis of HCNO and subsequent secondary chemistry. Possible chemistry involved was discussed in our previous publication.² To obtain product yields from the title reaction, product yields obtained from HCNO/buffer gas mixtures were subtracted from those obtained with the full ICN/HCNO buffer gas mixtures. This approach assumes that the secondary chemistry is not greatly affected by the presence or absence of the ICN precursor. Although this assumption is probably not perfect, we believe that it is sufficient for the purposes of this study, i.e., the identification of the major product channels of the title reaction.

Transient signals for CO were observed upon photolysis of

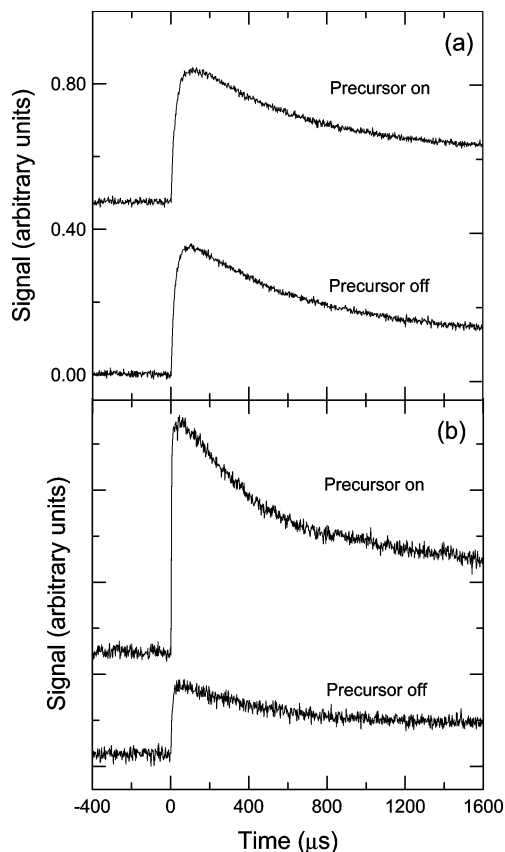
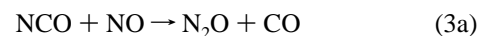


Figure 5. Transient signals of (a) CO and (b) NO. Reaction conditions: $P(\text{ICN}) = 0$ Torr (lower traces), $P(\text{ICN}) = 0.10$ Torr (upper traces), $P(\text{HCNO}) = 0.20$ Torr, $P(\text{CF}_4) = 1.0$ Torr (for CO transient only), $P(\text{SF}_6) = 1.0$ Torr (for NO transient only).

ICN/HCNO/CF₄ mixtures; however, nearly identical signals were observed upon photolysis of HCNO/CF₄ mixtures, as shown in Figure 5a. This indicates that most of the CO originates from background sources such as HCNO photolysis and resulting secondary chemistry, and it indicates that direct formation of CO in channels 1a, 1i, 1j, and 1k are not major product channels. We estimate a total upper limit of $\varphi_{1a} + \varphi_{1i} + \varphi_{1j} + \varphi_{1k} < 0.12$.

As shown in Figure 5b, a large transient signal for nitric oxide, NO, was detected upon 248 nm photolysis of ICN/HCNO/SF₆ mixture, while much smaller amounts were produced when the ICN precursor was omitted. We attribute this to nitric oxide formation by channel 1c.

In principle, NCO formed in channel 1d or via secondary chemistry could be probed directly by infrared absorption. Quantification is rather difficult, however, because of rather low infrared absorption coefficients and the reactivity of this species. A preferred procedure was to include nitric oxide in the reaction mixture, in order to convert NCO into stable products with high IR absorbance:



Branching ratios (at 296 K) of $\varphi_{3a} = 0.44$ and $\varphi_{3b} = 0.56$ have been reported.¹⁹ Large transient signals of N₂O and CO were detected upon 248 nm photolysis of ICN/HCNO/NO/buffer gas mixture and HCNO/NO/buffer gas mixture (SF₆ for N₂O detection and CF₄ for CO detection). Figure 6a shows the N₂O signals. There are significant differences between the signals

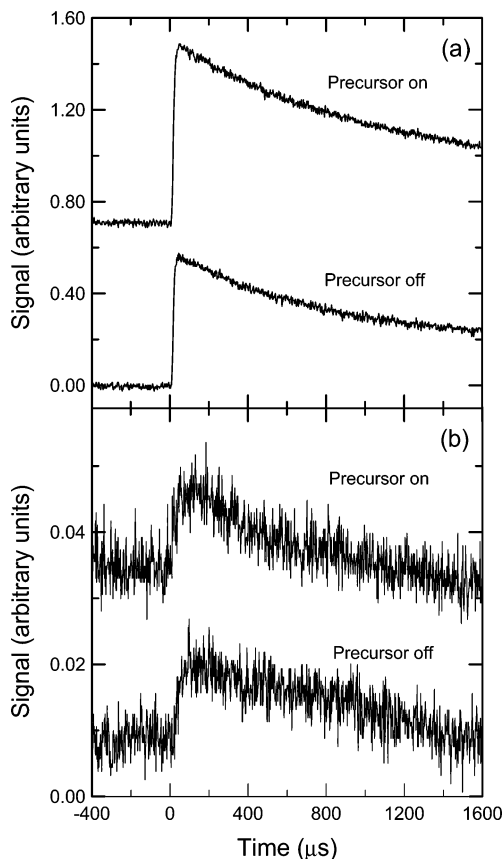
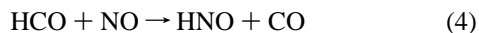


Figure 6. Transient signals of (a) N_2O and (b) HNO in the presence of NO . Reaction conditions: $P(\text{ICN}) = 0$ Torr (lower traces), $P(\text{ICN}) = 0.10$ Torr (upper traces), $P(\text{HCNO}) = 0.20$ Torr, $P(\text{NO}) = 2.0$ Torr, $P(\text{SF}_6) = 1.0$ Torr.

obtained with and without ICN, although a substantial background from HCNO photolysis is present. We attribute this additional N_2O and CO formation to production of NCO followed by reaction 3a. As we will show below, however, most or all of this NCO is not a direct product from channel 1d but is produced by secondary chemistry.

No transient signals for HCCO was observed upon 248 nm photolysis of $\text{ICN}/\text{HCNO}/\text{SF}_6$, indicating that channel 1e is not significant. We are unable to reliably estimate an upper limit because the infrared absorption coefficients of HCCO are unknown. Preliminary measurements in our laboratory indicate that the $\text{HCCO} + \text{HCNO}$ reaction is quite slow, so if HCCO is formed in significant quantities, we would expect to be able to detect it.

HCO products were not directly probed, but an HNO transient signal was detected upon 248 nm photolysis of an $\text{ICN}/\text{HCNO}/\text{NO}/\text{SF}_6$ mixture. HNO is presumably formed by the reaction



However, this signal is almost same as that obtained from 248 nm photolysis of $\text{HCNO}/\text{NO}/\text{SF}_6$ mixture. Because the HNO signal is the same with and without ICN, we conclude that most of the HCO originated from HCNO photolysis and/or subsequent secondary chemistry and not from channel 1f of the title reaction.

C_2N_2 is not detectable in our diode laser spectroscopy because of the lack of available laser diodes in their significant spectral region. As a result, we cannot probe the importance of channel 1b by transient infrared spectroscopy. We have, however, obtained static FT-IR spectra of the reaction mixture before and after extensive photolysis (1000 Excimer laser pulse). The stable

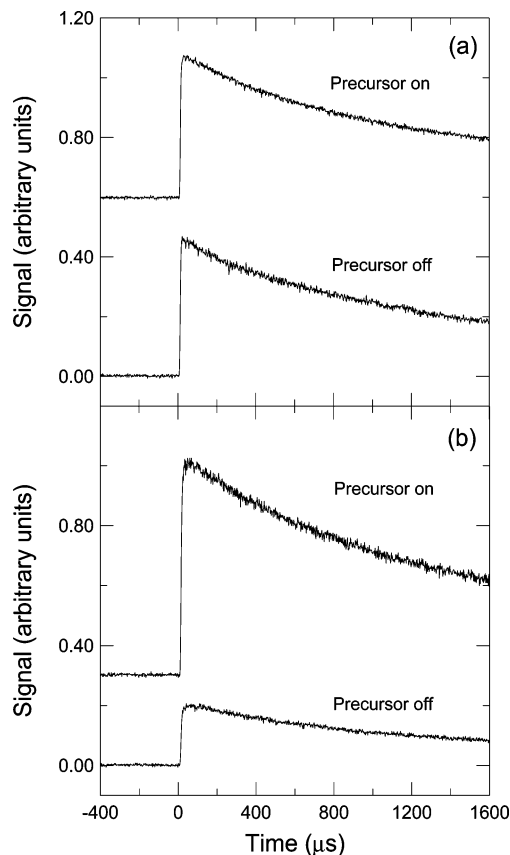


Figure 7. Transient signals of (a) $^{16}\text{O}^{12}\text{C}^{18}\text{O}$ and (b) $^{18}\text{O}^{12}\text{C}^{18}\text{O}$ in the presence of $^{15}\text{N}^{18}\text{O}$. Reaction conditions: $P(\text{ICN}) = 0$ Torr (lower traces), $P(\text{ICN}) = 0.10$ Torr (upper traces), $P(\text{HCNO}) = 0.20$ Torr, $P(^{15}\text{N}^{18}\text{O}) = 2.0$ Torr, $P(\text{SF}_6) = 1.0$ Torr.

TABLE 1: Product Yields of Reaction $\text{CN} + \text{HCNO}$

product	without ICN ^a	with ICN ^a	difference ^{a,b}	rel. yield ^c
NO	5.71	19.0	13.3	1
CO	9.22	11.06	1.84	0.139
CO^d	21.52	24.29	2.77	0.209
N_2O^d	5.82	8.83	3.01	0.226

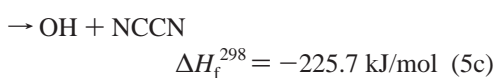
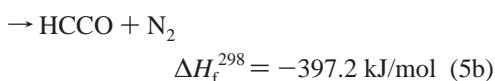
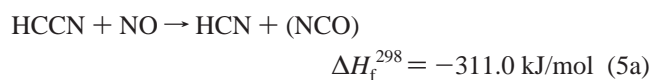
^a In units of 10^{12} molecule cm^{-3} . ^b Difference obtained by subtracting column 3 (yield with ICN) by column 2 (yield without ICN). ^c Difference yields (column 4) normalized to $[\text{NO}] = 1.00$. ^d Yields obtained in the presence of 2.0 Torr of NO .

products observed in the transient experiments are observable in the FT-IR, but no C_2N_2 was detected. Furthermore, any OH produced in channel 1b would be expected to react with HCNO , producing large amounts of CO^2 . Our lack of evidence for CO production (described above) suggests that channel 1b is not a major product channel. We estimate an upper limit of $\varphi_{1b} < 0.20$.

Transient signal amplitudes (peak–peak) of NO , N_2O , and CO were converted into absolute concentration using HITRAN line-strengths as described in a previous publication.¹⁹ Table 1 shows a typical dataset of product molecule yields. Shown are concentrations obtained both with and without the ICN precursor, and the difference between these two measurements. The right-hand column of Table 1 shows the resulting relative product yield.

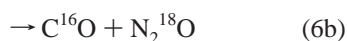
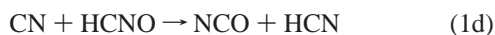
Table 1 shows that large amounts of N_2O and CO molecules are produced from photolysis of $\text{ICN}/\text{HCNO}/\text{NO}/\text{SF}_6$, which can be attributed to NCO formation as mentioned above. In

principle, other sources of these products could exist, such as CO formation from the reaction of HCCO with NO. If this reaction were important, however, we would expect an excess of CO. Our observation of nearly identical [CO] and [N₂O] yields is fairly strong evidence that reaction 3 is primarily responsible for the formation of these products. Employing the known branching ratio of reaction 3, we can estimate the yield of NCO to be [N₂O]/0.44. This results in an [NO]:[NCO] ratio of 1:0.51. Similarly, one can use CO yields to reach the same conclusion (since the CO and N₂O yields are approximately equal). Based on these data, one is tempted to conclude channel 1d is a significant product channel. However, given our observation of large amounts of NO products attributed to reaction 1c, we must also consider secondary chemistry of the HCCN molecule that is also produced. Under ICN/NO/HCNO/buffer gas conditions, the following reaction is expected to be significant:



The reaction has been studied by Curl et al.²⁰ Several other product channels may be written as well. Curl et al. reported detection of HCN and HCNO products. They attribute the HCN products to channel 5a. HCNO is unlikely to be formed directly in reaction 5, as this would be endothermic (it is the reverse of our channel 1c). Curl et al. proposed several possible secondary routes to HCNO formation. An additional route that they did not consider was channel 5b followed by the reaction of HCCO + NO. Although quantitative branching ratios were not reported in their study, it does appear very likely that reaction 5a is a major product channel. As a result, we cannot rule out the possibility that some or all of the NCO produced in our experiments originated from reaction 5a rather than 1d.

To determine the origin of NCO, we performed experiments with isotopically labeled ¹⁵N¹⁸O (only the oxygen labeling is relevant to this discussion). If NCO is produced directly in reaction 1d, ¹⁶OC¹⁸O and C¹⁶O would be produced upon 248 nm photolysis of an ICN/HCNO/¹⁵N¹⁸O/buffer mixture:



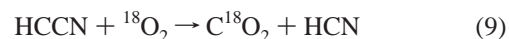
The isotopic labeling in the products of channel 6a is definite. The labeling in 6b is based on the assumption that this reaction proceeds via a straight-chain O–N–N–C–O intermediate, followed by N–C bond fission to form the products. Some rather difficult rearrangements would be necessary to put the ¹⁸O atom on the CO product. This assumption is supported by ab initio studies on this reaction.²¹ On the other hand, if NCO was produced from the secondary reaction 5a, ¹⁸OC¹⁸O and C¹⁸O molecules would be produced upon 248 nm photolysis of an ICN/HCNO/¹⁵N¹⁸O/buffer mixture:



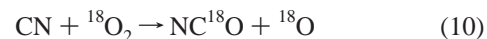
The ratio of ¹⁸OC¹⁸O to ¹⁶OC¹⁸O is therefore a sensitive test of the origin of the NCO radicals, with the caveat that we must still measure the difference in yields obtained with and without the ICN precursor, in order to subtract the yields of HCNO photolysis products.

The results of the isotopic labeling experiment are shown in Figure 7 and especially Table 2. Large yields of both ¹⁸OC¹⁸O and ¹⁶OC¹⁸O are observed upon photolysis of an ICN/HCNO/¹⁵N¹⁸O/SF₆ mixture; however, almost all of the ¹⁶OC¹⁸O signal is background, probably due to NCO produced by HCNO photolysis. Virtually none of the ¹⁸OC¹⁸O signal is background. After subtracting the photolysis background, we obtain a ratio of [¹⁸C¹²C¹⁸O]/[¹⁶O¹²C¹⁸O] = 6.01. As a result, we conclude that most of the NCO (other than HCNO photolysis background) is formed by secondary chemistry such as reaction 5a, and that direct formation of NCO by the title reaction in channel 1d is not significant. A similar conclusion can be reached from a comparison of C¹⁸O and C¹⁶O yields, but this experiment was less conclusive than the CO₂ experiment because of large photolysis backgrounds.

The isotopically labeled N¹⁸O experiment above provides fairly strong evidence for production of HCCN products in the title reaction, although we cannot directly detect HCCN in these experiments. Further evidence for HCCN formation is provided by the following experiment: If isotopically labeled ¹⁸O₂ is included (i.e., an ICN/¹⁸O₂/HCNO/SF₆ mixture is photolyzed), the following reaction is expected to occur:



The reaction of HCCN with O₂ has been studied previously,²⁰ with a reported rate constant of $1.8 \times 10^{-12} \text{ cm}^3 \text{ molec}^{-1} \text{ s}^{-1}$ and with CO₂ + HCN (or HNC) the only products identified. If ¹⁸O₂ and HCNO pressures are comparable, some of the CN radicals will react with ¹⁸O₂ to make primarily NC¹⁸O + ¹⁸O, and reactions of NC¹⁸O with HCNO may form CO₂; however, these products are expected to be of the mixed isotope ¹⁶O¹²C¹⁸O:



The rate of reaction 10 is $k_{10} = 2.4 \times 10^{-11} \text{ cm}^3 \text{ molec}^{-1} \text{ s}^{-1}$ at 298 K,²² while no literature reports exist for k_{11} . Note that CO₂ + HCNN is only one of many possible product channels of reaction 11, which will be the subject of an upcoming paper. The result of this experiment is that we detected $6.84 \times 10^{12} \text{ molec/cm}^3$ of ¹⁸O¹²C¹⁸O upon photolysis of an HCNO/ICN/

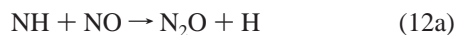
TABLE 2: ¹⁶O¹²C¹⁸O and ¹⁸O¹²C¹⁸O Yields in Secondary Reaction of CN + HCNO with ¹⁵N¹⁸O

product	without ICN ^a	with ICN ^a	difference ^{a,b}	rel. yield ^c
¹⁶ O ¹² C ¹⁸ O	3.129	3.495	0.365	0.166
¹⁸ O ¹² C ¹⁸ O	0.726	2.919	2.193	1

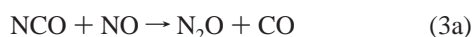
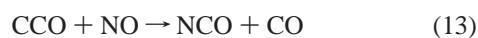
^a In units of 10¹² molecule cm⁻³. ^b Difference obtained by subtracting column 3 by column 2. ^c Difference yields (column 4) normalized to [¹⁸O¹²C¹⁸O] = 1.00.

$^{18}\text{O}_2/\text{SF}_6$ mixture while only 1.3×10^{12} molec/cm³ of $^{18}\text{O}^{12}\text{C}^{18}\text{O}$ as background was detected upon photolysis of $\text{HCNO}/^{18}\text{O}_2/\text{SF}_6$ mixture. Although we do not attempt to obtain quantitative branching ratio information from these yields, our observation of significant amounts of $^{18}\text{O}^{12}\text{C}^{18}\text{O}$ is certainly consistent with HCCN formation followed by reaction 9.

Two other possible product channels of the title reaction deserve mention. If channel (1g) was significant, we would expect to observe more N_2O yield than CO yield with 248 nm photolysis of $\text{ICN}/\text{HCNO}/\text{NO}/\text{buffer}$ gas, because the secondary reaction of NH with NO will produce additional N_2O .



N_2O is a major product of reaction 12, with $\varphi_{12\text{a}} = 0.77$.²³ Conversely, if channel 1h were significant, we would expect to observe more CO than N_2O upon photolysis of $\text{ICN}/\text{HCNO}/\text{NO}/\text{buffer}$ gas, because of the following reaction sequence:²⁴



In fact, we only measure approximately equal yields of N_2O and CO products upon 248 nm photolysis of $\text{ICN}/\text{HCNO}/\text{NO}/\text{buffer}$ gas. This is consistent with our assumption that N_2O and CO originate from reaction 3.

As a result of the above discussion, we conclude that 1c is the major product channel of the title reaction.

4. Discussion

Our results represent the first study of the title reaction. This is a very fast reaction with slight temperature dependence. An extrapolation of our measurement to the temperature range $T = 1200\text{--}1500$ K relevant in NO -reburning suggests a rate constant approximately half of our 298 K value, although clearly such an extrapolation is not warranted by the narrow temperature range of our data.

Several experimental artifacts can cause systematic errors in a pseudo-first-order kinetics experiment. The first, decomposition of HCNO sample during the experiment, was minimized by completing a single CN LIF decay measurement in about 5 min (typically, this allows 4 min for filling the cell and allowing the reagents to mix and 1 min for the LIF data collection). In this amount of time, less than 10% decomposition occurs. A related issue is the possible reaction of CN radicals with decomposition products, photoproducts, or reaction products from the title and/or secondary reactions. By using an estimated absorption cross section of HCNO at 248 nm of 1.41×10^{-19} cm², and assuming a photolysis quantum yield of unity, we estimated $\sim 4 \times 10^{12}$ cm⁻³ of HCNO photolysis products from a 4 mJ excimer pulse at $P(\text{HCNO}) = 0.05$ Torr (the highest pressure used in Figure 3). This is substantially less than our estimated $[\text{CN}]$ values of $\sim 2 \times 10^{13}$ cm⁻³ but furthermore represents only approximately 0.3% conversion of the initial HCNO . Because our measured rate constant is within an order of the gas kinetic, the reaction of CN with transient species produced by HCNO photolysis is clearly not a severe problem. If k_1 were several orders of magnitude slower, such secondary chemistry would be a more serious issue. Another issue is the possible reaction of CN with stable products, which could potentially build up over the ~ 100 shots required to obtain one

of the data sets of Figure 1. A simple test for this effect is to measure the CN decay twice in rapid succession on the same gas fill. If the CN reaction with stable products was a significant problem, we would expect the second measurement to yield a different value for the pseudo-first-order CN decay rate. In fact, we observed no change in the CN decay rate from two successive measurements on the same gas fill.

In addition to the product channels listed, one can write numerous other possibilities, for example involving formation of CNO rather than NCO , formation of HNC rather than HCN , etc. We cannot completely rule out CNO formation, except to note that it likely would be formed with enough internal energy to isomerize to the more stable NCO species. No evidence for HNC formation was observed in FTIR spectra taken. One can also write channels such as $\text{CN} + \text{HCNO} \rightarrow \text{CN} + \text{HNCO}$, which are exothermic because HNCO is the more stable isomer. Although we did not investigate this possibility in detail, we note that if such a channel were important, we would not observe the rapid CN disappearance apparent in our data.

No ab initio studies of the potential energy surface of this reaction have been reported. We can therefore only speculate regarding details of the reaction mechanism. Our observation of channel 1c as the only major product channel suggests a rather simple mechanism in which CN attack at the carbon atom of HCNO forms an $\text{HC}(\text{CN})\text{NO}$ complex, which then directly dissociates by $\text{C}\text{--}\text{N}$ bond fission to form $\text{HCCN} + \text{NO}$. A complete potential surface would show other structures and probably numerous possible rearrangements; however, our experimental results suggest that other pathways are higher in energy and are not significant.

5. Conclusion

The kinetics and product of the $\text{CN} + \text{HCNO}$ reaction were studied using laser-induced fluorescence and IR diode laser absorption spectroscopy. The reaction is very fast, with $k_1 = (1.04 \pm 0.10) \times 10^{-10}$ cm³ molec⁻¹ s⁻¹ at 298 K, and has a slight, negative temperature dependence. The major product channel is $\text{NO} + \text{HCCN}$.

Acknowledgment. This work was supported by the Division of Chemical Sciences, Office of Basic Energy Sciences of the Department of Energy, Grant DE-FG03-96ER14645.

References and Notes

- (1) Miller, J. A.; Klippenstein, S. J.; Glarborg, P. *Combust. Flame* **2003**, *135*, 357.
- (2) Feng, W. Meyer, J. P.; Hershberger, J. F. *J. Phys. Chem. A* **2006**, *110*, 4458.
- (3) Chase, M. W. NIST-JANAF Thermochemical Tables. *J. Phys. Chem. Ref. Data* **1998**; 4th ed.
- (4) Schuurman, M. S.; Muir, S. R.; Allen, W. D.; Schaefer, H. F., III. *J. Chem. Phys.* **2004**, *120*, 11586.
- (5) Clifford, E. P.; Wenthold, P. G.; Lineberger, W. C.; Petersson, G. A.; Broadus, K. M.; Kass, S. R.; Kato, S.; Depuy, C. H.; Bierbaum, V. M.; Ellison G. B. *J. Phys. Chem. A* **1998**, *102*, 7100.
- (6) Osborn, D. L.; Mordaunt, D. H.; Choi, H.; Bise, R. T.; Neumark, D. M.; Rohlfling, C. M. *J. Chem. Phys.* **1997**, *106*, 10087.
- (7) Francisco, J. S.; Liu R. *J. Chem. Phys.* **1997**, *107*, 3840.
- (8) Choi, H.; Mordaunt, D. H.; Bise, R. T.; Taylor, T. R.; Neumark, D. M. *J. Chem. Phys.* **1998**, *108*, 4070.
- (9) Pasinski, T.; Kishimoto, N.; Ohno, K. *J. Phys. Chem.* **1999**, *103*, 6746.
- (10) Wentrup, C.; Gerecht, B.; Briehl, H. *Angew. Chem., Int. Ed. Engl.* **1979**, *18*, 467.
- (11) Wilmes, R.; Winnewisser, M. *J. Labelled Compd. Radiopharm.* **1993**, *33*, 157.
- (12) Rothman, L. S.; et al. *J. Quant. Spectrosc. Radiat. Transfer* **1992**, *48*, 469.
- (13) Cerny, D.; Bacis, R.; Guelachvili, G.; Roux, F. *J. Mol. Spectrosc.* **1978**, *73*, 154.

- (14) Davies, P. B.; Hamilton, P. A. *J. Chem. Phys.* **1975**, *76*, 2127.
(15) Johns, J. W. C.; McKellar, A. R. W.; Weinberger, E. *Can. J. Phys.* **1983**, *61*, 1106.
(16) Ferretti, F. L.; Rao, K. N. *J. Mol. Spectrosc.* **1974**, *51*, 97.
(17) Unfried, K. G.; Glass, G. P.; Curl, R. F. *Chem. Phys. Lett.* **1991**, *177*, 33.
(18) Cooper, W. F.; Hershberger, J. F. *J. Phys. Chem.* **1992**, *96*, 771.
(19) Cooper, W. F.; Park, J.; Hershberger, J. F. *J. Phys. Chem.* **1993**, *97*, 3283.
(20) Adamson, J. D.; Desain, J. D.; Curl, R. F.; Glass, G. P. *J. Phys. Chem. A* **1997**, *101*, 864.
(21) Lin, M. C.; He, Y.; Melius, C. F. *J. Phys. Chem.* **1993**, *97*, 9124.
(22) Baulch, D. L.; Cobos, C. J.; Cos, R. A.; Frank, P.; Hayman, G.; Just, Th.; Kerr, J. A.; Murrells, T.; Pilling, M. J.; Troe, J.; Walker, R. W.; Warnatz, J. *J. Phys. Chem. Ref. Data* **1994**, *23* (Suppl. 1), 847.
(23) Quandt, R. W.; Hershberger, J. F. *J. Phys. Chem.* **1995**, *99*, 16939.
(24) Thweatt, W. D.; Erickson, M. A.; Hershberger, J. F. *J. Phys. Chem. A* **2004**, *108*, 74.